Colloid Polym Sci 280: 7–17 (2002)

ORIGINAL CONTRIBUTION

N. Grozev
A. Svendsen
R. Verger
I. Panaiotov

Enzymatic hydrolysis by *Humicola lanuginosa* lipase of polycaprolactone monolayers

Received: 25 July 2000
Revised: 28 November 2000
Accepted: 29 November 2000

N. Grozev · I. Panaiotov (✉)
Biophysical Chemistry Laboratory
University of Sofia
J. Bourchier st. 1
1126 Sofia, Bulgaria

A. Svendsen
Novo Nordisk, Enzyme Design
Novo Alle, 2880 Bagsvaerd, Denmark

R. Verger
ERS 26 "Lypolyse enzymatique" du
Centre National de la Recherche
Scientifique, B.P.71, 13402 Marseille
Cédex 9, France

Abstract The enzymatic hydrolysis by *Humicola lanuginosa* lipase (HLL) of spread insoluble monolayers of polycaprolactone with various molecular weights was studied by measuring the decrease in surface area and in surface potential, in a barostat surface balance. The interfacial hydrolysis under the action of enzymes leads to the progressive fragmentation of the polymer molecules and to the appearance at the interface of charged insoluble and small soluble products. The solubilization of the small soluble fragments was detected by measuring the decrease in surface area during hydrolysis. An independent study showed that, in contrast to poly(lactic-*co*-glycolic acid) (PLAGA) oligomers, this solubilization is not instantaneous. Taking into account the solubilization rates, one can determine the kinetics of enzymatic hydrolysis. The specific catalytic activity of HLL was estimated in the framework of the random-scission model and compared to those obtained for the hydrolysis of monolayers built up of PLAGA or of simple di- and triglyceride molecules.

Keywords Polycaprolactone · Spread monolayer · Enzymatic hydrolysis · *Humicola lanuginosa* lipase

Introduction

During the last two decades, the role of various factors in the degradation of polyester microparticles, used as controlled release systems, has been investigated extensively [1–15].

The modelling of the particle erosion is a difficult task [13–15] since numerous physicochemical processes are involved in the erosion of the polymer matrix of microparticles. The hydrolysis and scission of ester bonds are of utmost importance for the complex degradation process. The hydrolytic reaction takes place at the polymer–water interface where the scission of ester bonds is coupled with various interfacial phenomena, such as mass transfer of the reactant products, interfacial accumulation of charged hydrolytic insoluble products, desorption and solubilization of low-molecular-weight oligomers, etc.

In order to analyse the mechanisms of hydrolysis, some simple model systems – dilute polymer bulk solution [16] and polymer monolayer at the air–water interface [17] – are proposed.

The monolayer approach is characterized by the ability to control and modify the interfacial organization of the substrate by varying the surface pressure. In this way, one can achieve the optimal chain conformation for hydrolytic attack, i.e., monomers closely packed at the interface, with all their ester bonds accessible to the underlying aqueous phase containing the enzyme.

In previous works [18, 19], the influence of the molecular weight and chemical composition on the hydrolysis of poly(lactic acid) and poly(lactic-*co*-glycolic acid) (PLAGA) was shown and it was concluded that the hydrolysis rate is higher for samples rich in glycolic acid, with a low degree of polymerization, at a surface pressure corresponding to the optimal interfacial orga-

nization of the units. In this article, the results obtained for the hydrolysis of polycaprolactone (PCL) are presented.

There were several reasons for choosing PCL as a subject of our investigation:

1. To get an insight into the effect of the hydrocarbon chain length on the interfacial hydrolysis rate and the solubilization rate of the water-soluble fragments (in Refs. [18, 19], this solubilization is assumed to take place practically immediately).
2. The possibility to use lower-molecular-weight polycaprolactondiols (PCLD) (precursors in the formation of PCL) in order to test independently the solubilization rate of small water-soluble fragments.
3. To ascertain which mode of bond scission (random or end) is more plausible.

Materials and methods

Materials

The polymers used in this work (Fig. 1) were supplied by Aldrich (Steinheim, Germany). The molecular weights (M_n), determined by size-exclusion chromatography and the polymolecularity index (I) for the PCL samples were $M_n = 80{,}000$ ($I = 1.5$), $M_n = 42{,}500$ ($I = 1.5$) and $M_n = 10{,}000$ ($I = 1.4$). The polymolecularity indexes for PCLD were not available.

Tris(hydroxymethyl)aminomethane (Tris), used in the buffer solution (Tris/HCl) with pH 8 was supplied by Merck (Darmstadt, Germany). HCl was purchased from Theokom (Sofia, Bulgaria) and was used without further purification. Dichloromethane (DCM) was supplied by Fluka. In all experiments, doubly distilled water was used.

Humicola lanuginosa lipase (HLL) (active form) and HLL-S146A (mutant form) were generous gifts from Novo Nordisk (Denmark).

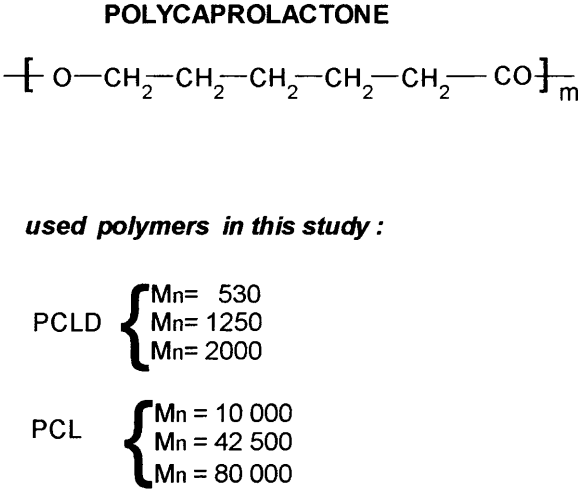

Fig. 1 Chemical formulae of polycaprolactones (*PCLs*) used as an enzymatic substrate

Measurements at the air–water interface

The monolayers of PCL were spread on the aqueous subphases from a volatile DCM solution ($c = 1$ g dm^{-3}) using an Exmire microsyringe. DCM was found to be a good solvent leading to a defolding of polymer chains and to the formation of a more unfolded structure at the air–water interface [20].

The surface pressure (π) was measured using a KSV-2200 (Finland) surface balance equipped with a platinum plate. The surface potential (ΔV) was measured simultaneously by using a gold-coated ^{241}Am ionizing electrode, a reference electrode and a KP 511 (Kriona, Bulgaria) electrometer, connected to a personal computer provided with user software for real-time data measurements. As usual, the surface potential of the pure aqueous surface fluctuated for about 30 min. When the air–water interface became constant, spreading of the monolayer could be performed. The accuracy of the initial surface potential value was ± 15 mV; however, the accuracy of the rate of surface potential variation, $d\Delta V/dt$, was 1 mVs^{-1}.

Three kinds of experiments were performed:

1. Surface pressure–area and surface potential–area isotherms were obtained after spreading the DCM solution of the polyester on the aqueous subphase at neutral pH on the maximum available area of the KSV-2200 surface balance. The values of the surface pressure after spreading were less than 0.5 m Nm^{-1}. The monolayers were then compressed at a constant velocity of 10 cm^2 min^{-1}.
2. The decrease of the surface area (ΔA) and that of the surface potential (ΔV) as a function of time were measured simultaneously during the hydrolysis of the PCL and PCLD monolayers at constant surface pressure by using an automatic barostat KSV-2200 surface balance. A "zero-order" trough [21], composed of a reaction compartment with area $A' = 50$ cm^2 and a reservoir compartment with area A″, communicating by means of a narrow surface channel (area 0.25 cm^2), was used (Fig. 2). After spreading over the maximum available area (320 cm^2), the polyester monolayers were compressed at a constant velocity of 100 cm^2 min^{-1} to a given value of the surface pressure, and the barostat setup was switched on. The corresponding area is denoted A_{ini}. Then the HLL enzyme was injected in the buffer subphase (pH 8) in the reaction compartment and stirred continuously (magnetic stirrer, 250 rpm). The aqueous subphase in the reservoir compartment was maintained at neutral pH.
3. In the same way, the decrease of the surface area and that of the surface potential as a function of time were measured at

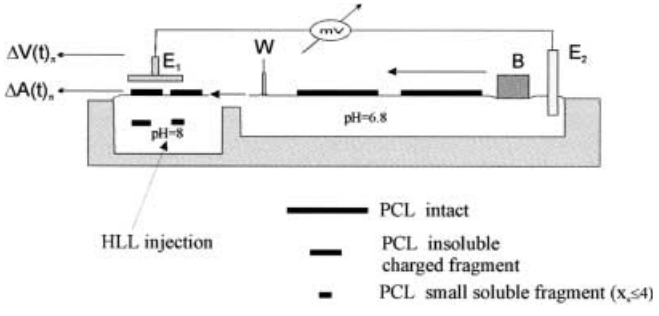

Fig. 2 Scheme of "zero-order" trough used for measurements during the interfacial hydrolysis. The trough is composed of a reaction compartment (A' with surface area 50 cm^2) and a reservoir compartment (A'' – 270 cm^2) communicating by means of a narrow surface channel (width 0.5 cm) B – barrier; W – Wilhelmy plate; E_1 – ionizing electrode; E_2 – reference electrode; *HLL* – *Humicola lanuginosa* lipase

constant surface pressure during the solubilization of lower-molecular-weight PCLD monolayers spread on the same buffer subphase without enzyme injection. Solubilization was also followed without stirring.

Molecular models

Molecular models were created by using the program Chem3D Pro, version 3.5.1, based on Norman L. Allinger's MM2 force field.

Theoretical model

Interfacial hydrolysis of linear polymer chain under barostatic conditions

The hydrolysis kinetics of the spread monolayers of PCL with different molecular weights were followed by measuring simultaneously the decrease in the surface area, ΔA, with time as well as the evolution of the surface potential, $\Delta V(t)$, under barostatic conditions.

The decrease $\Delta A(t)$ of the surface area is due to the fragmentation of the linear polymer chain, the progressive appearance of water-soluble oligomers (of up to four repeat units) and monomers and to their solubilization in the aqueous subphase with some finite rate.

The fragmentation is accompanied by the accumulation of large insoluble, negatively charged fragments at the interface. In fact, at each hydrolytic step, a net negative charge appears at the end of the polymer fragment (one per fragment). This could be detected by measuring the evolution of the surface potential ΔV with time.

For the process occurring under barostatic conditions, two forms of the mass conservation equation may be associated with the experimental data $\Delta A(t)$.

The first one describes the decrease in the area occupied by the monolayer in the course of the enzymatic hydrolysis

$$\Delta A(t) = A'\beta(t) + \sum_{i=0}^{i} \Delta A(t_i)\beta(t - t_i) - \Delta A_{\mathrm{enz}}(t) \quad , \qquad (1)$$

where β is the normalized decrease in the surface area, which can be deduced numerically from the experimental data $\Delta A(t)$. Assuming that the surface density of the monomers remains constant during the hydrolysis under barostatic conditions, β is the fraction of the solubilized monomers per polymer molecule and $\Delta A_{\mathrm{enz}}(t)$ is the variation of the area due to the penetration of enzyme molecules at the surface.

This equation is obtained by taking into account the progressive fragmentation and solubilization of the polymer molecules initially present in the reaction compartment (the term A') as well as the contribution of the i portions ($\Delta A_{t=t_i}$) continuously provided by the reservoir to the reaction compartment (Fig. 2).

The second mass conservation expression is associated with the accumulation of negative charges per unit area, $s^-(t)$,

$$s^-(t) = \frac{\Gamma_0}{A'}\left[A'\gamma(t) + \sum_{i=0}^{i} \Delta A(t_i)\gamma(t - t_i)\right] \quad , \qquad (2)$$

where Γ_0 is the surface density of monomer units, which remains constant during hydrolysis under barostatic conditions, and γ is the fraction of the charges situated at the end of the insoluble fragments, remaining at the interface, from the total number of ester bonds, s_0, in one polymer molecule.

The degree of completion, $\alpha(t)$, of the hydrolysis (the fraction of broken ester bonds) is given by the following expression:

$$\alpha(t) = 1 - \frac{s(t)}{s_0} \quad , \qquad (3)$$

where $s(t)$ and s_0 are the numbers of intact ester groups per square centimetre at time t and $t = 0$, respectively.

The use of Eq. (1) together with the experimental data $\Delta A(t)$ allows the calculation of the values of β at each moment t. Because β is connected with the degree of completion, $\alpha(t)$, one is able to calculate the latter.

In order to find the relationship between β and α, the mode of fragmentation of the linear polymer chain should be ascertained. Two limit modes of fragmentation can be considered:

1. A process of random fragmentation, based on the assumption that the reactivity of all ester groups is equivalent. By this mode, fragments with different lengths would appear with time. The number, ω_x, of fragments constituted by x monomers, obtained during the fragmentation of one polymer molecule with initial polymerization number $n_p \equiv s_0 + 1$ is given by

$$\omega_x(\alpha) = \alpha(1 - \alpha)^{x-1}[2 + (s_0 - x)\alpha] \quad . \qquad (4)$$

In this case, the fraction of solubilized small fragments (of up to four repeat units) is expressed by the following equation

$$\beta(\alpha) = \frac{\sum_{x=1}^{4} \omega_x(\alpha) x \delta_x(t)}{s_0 + 1} \quad , \qquad (5)$$

where $\omega_x x$ is the number of monomers attached to the soluble fragments at time t. If their solubilization in the aqueous subphase is not instantaneous, only some (δ_x) of them are solubilized at time t, while the part ($1–\delta_x$) remains at the interface. $\delta_x(t)$ takes into account the finite solubilization rate of the fragments with x (from one to four) repeat units. In the limit case of immediately solubilized small fragments,

$\delta_x = 1$. The values for $\delta_x(t)$ can be determined by an independent measurement of the rate of solubilization of model lower-molecular-weight molecules of PCLD (see Results and discussion).

In random scission mode, the following expression can be written for the fraction $\gamma(t)$ (the part of net charges remaining at the interface):

$$\gamma(\alpha) = \frac{\sum_{x=1}^{n_p} \omega_x(\alpha)(1-\delta_x)}{s_0} \quad . \tag{6}$$

2. End scission is the mode of fragmentation when only the chain end groups are hydrolysed and at each scission step only one unit is solubilized, so the number of solubilized units is equal to 1 multiplied by $s_0\alpha\delta_x$.

Thus, the fraction of solubilized fragments per polymer molecule is given by

$$\beta(\alpha) = \frac{s_0\alpha\delta_x}{s_0} = \alpha\delta_x \quad . \tag{7}$$

At each scission step only one charge remains at the end of the progressively shortened polymer molecule. Then, the fraction γ is given by

$$\gamma(t) = \frac{1}{s_0} = \text{constant} \quad . \tag{8}$$

By using the relationship between α and β in the framework of the two modes of fragmentation, Eqs. (5) and (7), and the mass conservation, Eq. (1), as well as the values obtained for δ_x by independent solubilization experiments, one could calculate the values of $\alpha(t)$ corresponding to the random or end mode of fragmentation.

By using the mass conservation (Eq. 2) and the expressions for γ (Eqs. 6 or 8), it is possible to obtain the expressions for the interfacial density of charges $s^-(t)$ per square centimetre in the framework of the two limit modes of fragmentation.

On the other hand, the interfacial density of charges $s^-(t)$ can be obtained on the basis of the simultaneously measured surface potential data $\Delta V(t)$, without any suppositions about the mode of fragmentation.

By comparing the values of $s^-(t)$ obtained from these two approaches, the mode of fragmentation could be established.

The interpretation of the $\Delta V(t)$ data is based on Schulman and Rideal's definition of the surface potential, ΔV, for charged monolayers as a sum of the contributions of the dipole moments and of the double layer of counterions [22],

$$\Delta V = 4\pi\mu_\perp\Gamma + \psi_0 \quad , \tag{9}$$

where $\mu_\perp \equiv \frac{\mu}{\varepsilon'}$ is the sum of vertical components of the dipole moments in one caproic unit, ε' is the dielectric constant in the plane of the monolayer, Γ is the surface density of units, remaining constant during the hydrolysis under barostatic conditions ($\Gamma = \Gamma_0$) and ψ_0 is the electrostatic potential in the plane of the interface relative to the subjacent aqueous phase, containing monovalent counterions. The initial value of ΔV at $t = 0$, before the appearance of charged units, is given by the Helmholtz equation:

$$\Delta V_0 = 4\pi\mu_\perp\Gamma_0 \quad . \tag{10}$$

The observed decrease in ΔV with time is related to the appearance of negatively charged products at the interface.

The most frequently used expression for ψ_0 is based on the Gouy–Chapman classical theory of the diffuse double layer:

$$\psi_0 = \frac{2kT}{e_0}\sinh^{-1}\left(\frac{e_0 s^-}{(2n_i\varepsilon kT/\pi)^{\frac{1}{2}}}\right) \tag{11}$$

and

$$\psi = \psi_0 e^{-\chi z} \quad , \tag{12}$$

where z is the distance from the plane charged surface, s^- is the charge per square centimetre of a plane, impenetrable, uniformly charged surface at $z = 0$, n_i is the concentration of the monovalent counterions in the bulk, presented as point charges, being able to approach the charged plane at $z = 0$, ε is the dielectric constant of water, k is the Boltzmann constant, T is the absolute temperature, e_0 is the electrostatic charge and $\chi^{-1} = \left(\frac{8\pi e_0^2}{\varepsilon kT} n_i\right)^{-1/2}$ is the Debye distance.

The electrical approach is based on the direct measurement of $\Delta V(t)$ at constant π and on the classical interpretation of the surface potential data (Eq. 9) as the sum of a positive contribution of the dipole moment of the carbonyl group and a negative contribution of the double layer of counterions. Assuming that the appearance of negatively charged units during the hydrolysis does not modify the dipole moment of the carbonyl group, and by using Eqs. (10) and (11), Eq. (9) becomes

$$\Delta V = 4\pi\mu_\perp\Gamma_0 - \frac{2kT}{e_0}\sinh^{-1}\left(\frac{e_0 s^-}{(2n_+\varepsilon kT/\pi)^{1/2}}\right) \quad . \tag{13}$$

From Eqs. (10) and (13), the corresponding Graham equation is given by

$$s^-(t) = \frac{1}{e_0}\sqrt{\frac{2n_+\varepsilon kT}{\pi}}\sinh\frac{e_0[\Delta V_0 - \Delta V(t)]}{2kT} \quad . \tag{14}$$

In the more realistic situation, when the negative charge modifies the positive dipole moment of the corresponding carbonyl group from $\mu_\perp$ to $\mu_\perp'$, the variation of ΔV with time is described by the following expression:

$$\Delta V(t) = 4\pi\mu_{\perp}(\Gamma_0 - s^-) + 4\pi\mu'_{\perp}s^- - \frac{2kT}{e_0}\sinh^{-1}\left(\frac{e_0 s^-}{(2n_+\varepsilon kT/\pi)^{1/2}}\right) \quad (15)$$

From Eqs. (10) and (15), one obtains the following form of the Graham equation:

$$s^-(t) = \frac{1}{e_0}\sqrt{\frac{2n_+\varepsilon kT}{\pi}}\sinh\frac{e_0\left[\Delta V_0 - \Delta V(t) + 4\pi\left(\mu'_{\perp} - \mu_{\perp}\right)s^-\right]}{2kT}. \quad (16)$$

Solubilization of small polymer fragments under barostatic conditions

Following the general concepts of the solubilization kinetics [23], the process consists of two consecutive steps: desorption through an energy barrier from the surface into the subsurface and diffusion from the latter into the bulk. If the process is controlled by the bulk diffusion stage, it can be described by the following well-known equation:

$$\ln A = \ln A_{\text{ini}} - \frac{2c_0}{\Gamma_0}\sqrt{\frac{D}{\pi}}\sqrt{t}\ , \quad (17)$$

where c_0 and Γ_0 are the bulk and surface concentrations at equilibrium and D is the bulk diffusion coefficient.

Results and discussion

State of the PCL monolayers spread at neutral pH

The surface pressure–area [$\pi(A)$] and surface potential–area [$\Delta V(A)$] isotherms were measured for all the polymers studied, spread at neutral pH. As an example, the isotherms $\pi(A)$ (curve 1) and $\Delta V(A)$ (curve 2) obtained for the monolayer of PCL with $M_n = 10{,}000$ are presented in Fig. 3. The inflection point observed at $\pi \sim 8$ mNm^{-1} and $A \sim 32$ Å^2 per monomer in the $\pi(A)$ isotherm corresponds to a saturation in the $\Delta V(A)$ isotherm and to close packing of all caproic units at the interface [24].

By using the Helmholtz equation with $\Delta V = 400$ mV, $\Gamma = 2.91 \times 10^{14}$ monomers cm^{-2} and the value of $\varepsilon' = 2$, typical of the polyethylene chains, a value of $\mu = 730$ mD for the monomer is obtained.

Figure 4 displays the probable interfacial disposition of a part of a PCL molecule, with two caproic units where the main-chain backbone tends to orient so that the polar parts (the carbonyl groups) interact predominantly with the aqueous phase, while the nonpolar hydrocarbon chain lies at the interface. The value of $A \sim 32$ Å^2 per monomer is in agreement with the calculated average area (34 Å^2) occupied by one unit (assumed as a circle with diameter 6.55 Å^2). The experimental value of $\mu = 730$ mD supports the concept that the most important contribution to the effective dipole moment is that of the dipole moment $\mu = 360$ mD

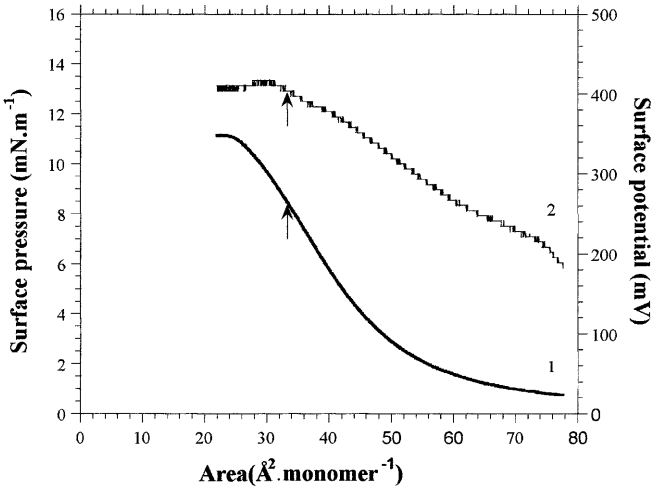

Fig. 3 Surface pressure–area [$\pi(A)$] (*curve 1*) and surface potential–area [$\Delta V(A)$] (*curve 2*) isotherms for a PCL ($M_n = 10{,}000$) monolayer spread at neutral pH. The *arrows* indicate the state in which all repeat units are close-packed

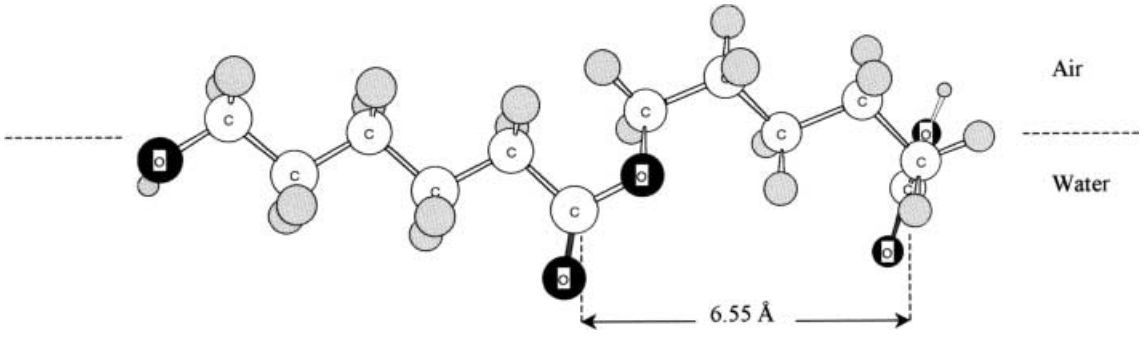

Fig. 4 Interfacial orientation of a part of the PCL molecule with two caproic units

of a carbonyl group anchored to the aqueous phase and that a second dipole moment, $\mu = 170$ mD, due to the orientation of C–O at the interface, is also present [22].

The phase transition observed at further compression was interpreted [24–26] as formation into the adjacent air phase of three-dimensional structures (loops) organized in microdomains. The plateau is situated at lower values of the interfacial pressure ($\pi = 11$ mNm^{-1}) and is more pronounced and longer than in the case of PLA50 ($\pi = 15$ mNm^{-1}) [17]. It is related to the presence of the hydrophobic chain C_5H_{10} in the caproic unit and to the stronger interactions at the interface.

The π(A) isotherms for all the polymers studied are presented in Fig. 5. It is seen that the inflection points are situated close to a value of $\pi = 9$ mNm^{-1} and practically there is no dependence on the chain length. The influence of the molecular weight is suggested by the formation of the three-dimensional structures – the longer the chain, the lower the corresponding value of π in the plateau.

Solubilization of lower-molecular-weight PCLD monolayers

The solubility of the series of accessible 1-, 4-, 11-, and 18-mers was studied. As an example, the decrease in the area with time under barostatic conditions (with and without stirring), after spreading the tetramer at the air–water interface, is presented in Fig. 6A. It should be noted that stirring does not affect the results.

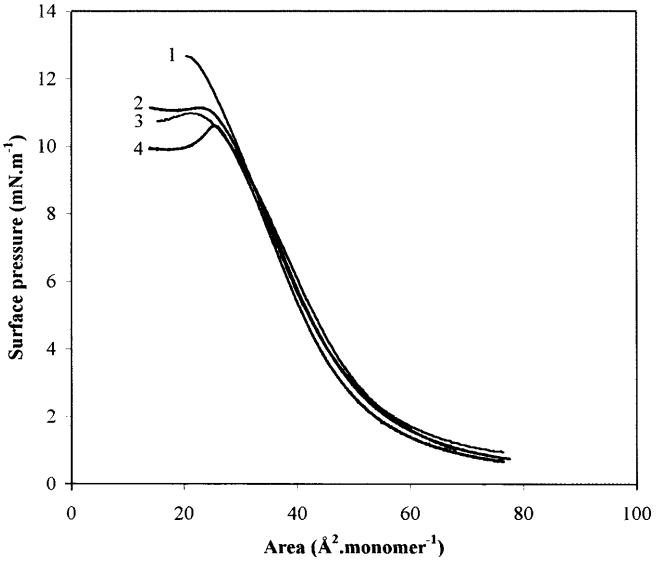

Fig. 5 $\pi(A)$ isotherms for PCL monolayers spread at neutral pH: *curve 1* – polycaprolactondiols (*PCLD*) ($M_n = 2000$); *curve 2* – PCL ($M_n = 10{,}000$); *curve 3* – PCL ($M_n = 42{,}500$); *curve 4* – PCL ($M_n = 80{,}000$)

At the beginning of the experiments ($t = 0$ and $A = A_{ini}$), a certain quantity of tetramers is spread. The total area, $A(t)$, of the monolayer decreases with time owing to the progressive solubilization of the tetramers. The solubilized part from 1 cm^2 at time t is given by

$$\delta(t) = \frac{\Delta A(t)}{A_{ini}} \quad . \tag{18}$$

The values for $\delta(t)$ are in the interval $0 \le \delta(t) \le 1$.

The relative solubilization rate, v_s, gives the solubilized part of PCLD per unit area per unit time:

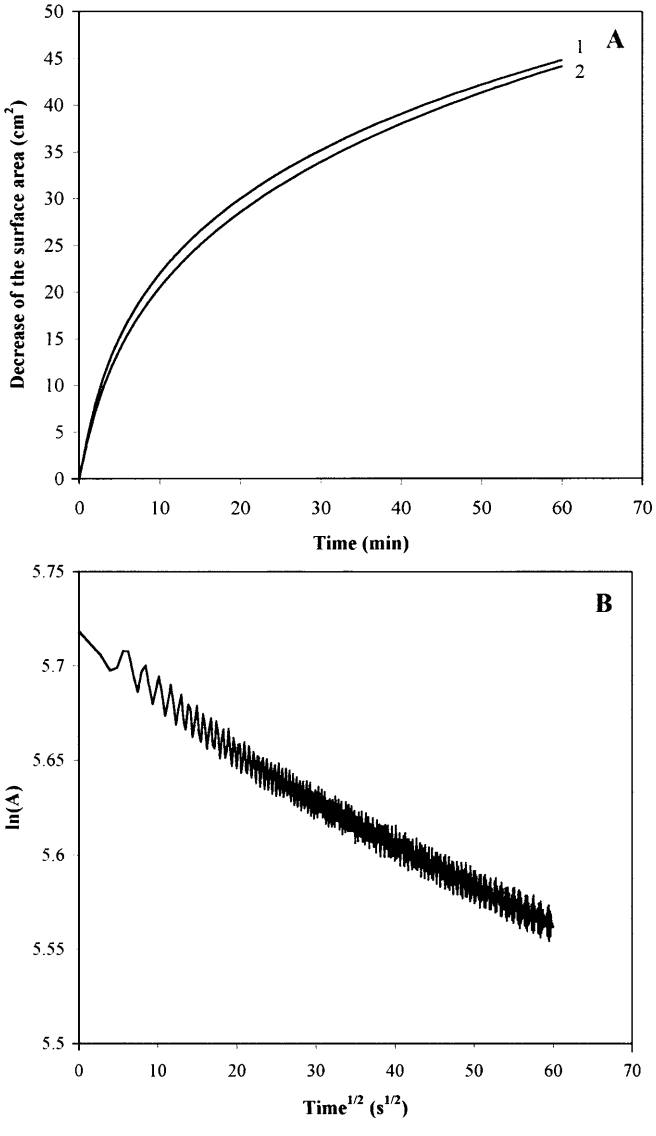

Fig. 6 **A** Decrease in the surface area (A) with time (t) due to the solubilization of the spread tetramers – PCLD ($M_n = 530$). *Curve 1* – with stirring, *curve 2* – without stirring the subphase. **B** Linearization of the data for the solubilization of tetramers on the scale $\ln A(\sqrt{t})$ in accordance with Eq. (17)

$$v_s = \frac{1}{A(t)}\frac{d(\Delta A)}{dt} \quad . \tag{19}$$

For small molecules, if the solubilization process is diffusion-controlled, the data in Fig. 6A must be linearized in the scale $\ln A(\sqrt{t})$, in accordance with Eq. (17). The results are presented in Fig. 6B. From the respective slope, a value of 45.5 for $\frac{\Gamma_0}{c_0\sqrt{Dt}}$ (at $t = 60$ s) is obtained. In this way, from the data $\Delta A(t)$ in Fig. 6A, the values for $\delta_4(t)$ for the tetramers studied can be derived by means of Eq. (18).

As the di- and tricaprolactones were not available for investigation of their solubility, the values of δ (t) for them were estimated by comparison with the data obtained previously [27] (Table 1) for fatty acids.

In Ref [27], $\frac{\Gamma_0}{c_0\sqrt{Dt}}$ is introduced as a criterion for the insolubility. The values of 9.90, 0.77 and 0.09 ($t = 60$ s) for lauric (C_{12}), capric (C_{10}) and caprylic (C_8) acids, respectively, were obtained and are presented in Table 1.

By linear extrapolation (the criterion for the insolubility of C_{12} is higher by 1 order of magnitude than for C_{10}, while, in turn, the criterion for the insolubility of the latter is about tenfold higher than that corresponding to C_8), it is possible to estimate the values for C_{13}, C_{11}, C_9 and C_7, also presented in Table 1.

The value obtained for the criterion for the insolubility of 45.5 in the case of the tetramer, allows one to assume that this PCLD corresponds to the fatty acid with 13 carbon atoms (C_{13}).

In order to estimate the solubility of the nonavailable tri- and dicaprolactone, the data for the fatty acids (Table 1) are used on the basis of the relationship between the amphiphilic structure of the molecules and their solubility. Let us introduce the ratio (φ_i) of the number of hydrophobic groups (n_{CH_2}) to the number of the hydrophilic ones (n_{hyd}) in the molecule:

$$\varphi_i = \frac{n_{CH_2}}{n_{hyd}} \quad . \tag{20}$$

The results for φ_i are easily obtained and are presented in Tables 1 and 2. From the values $\varphi_4 = 4$ and $\varphi_3 = 3.75$, it follows that φ for the trimer is lower by 6.25% than that of the tetramer. In the range of the fatty acids, the difference (in percent) in the values of φ_i is

Table 1 Values for the criterion for insolubility, $\frac{\Gamma_0}{c_0\sqrt{Dt}}$ (measured [27] and * estimated), as well as the values for the ratio $\varphi = \frac{n_{CH_2}}{n_{hyd}}$ for fatty acids

Fatty acid	φ_i	$\frac{\Gamma_0}{c_0\sqrt{Dt}}$
C_{13}	12	45*
C_{12}	11	9.9
C_{11}	10	3.3*
C_{10}	9	0.77
C_9	8	0.4*
C_8	7	0.09
C_7	6	0.009*

Table 2 The values for the ratio $\varphi_i = \frac{n_{CH_2}}{n_{hyd}}$ for the small soluble fragments

Polycaprolactone	φ_i
Tetramer	4
Trimer	3.75
Dimer	3.33
Monomer	2.5

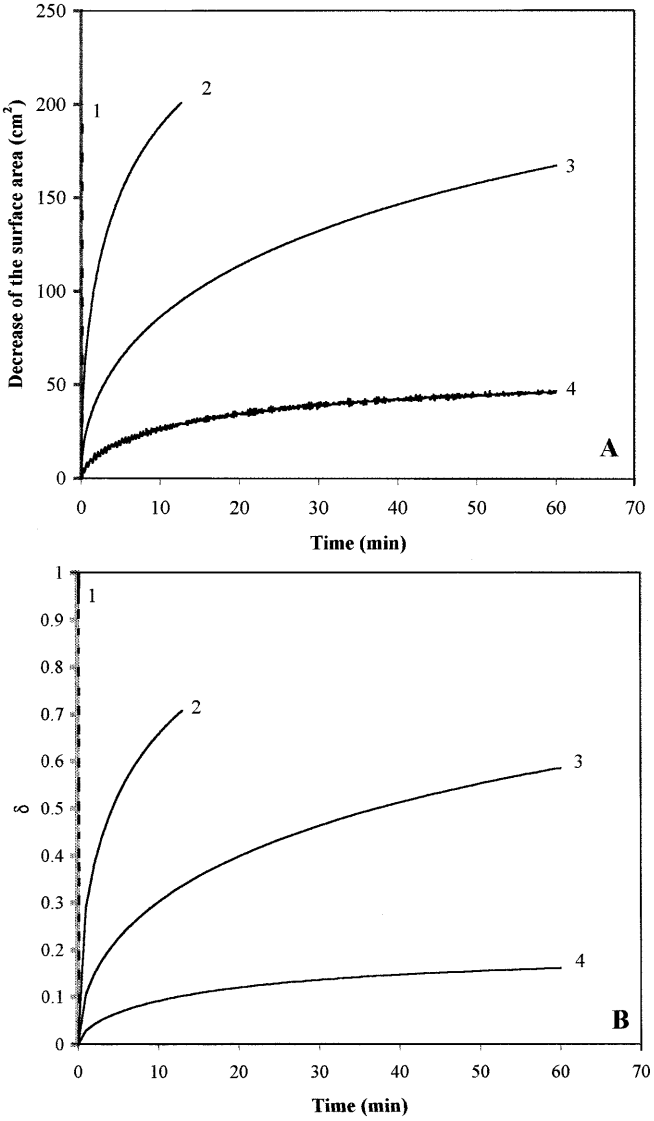

Fig. 7 **A** Decrease in the surface area (A) with time (t) for the small soluble products; *curve 1* – real measurement for caprolactone (monomer); *curve 2* – curve reconstructed by using Eq. (17) for the dimer; *curve 3* – curve reconstructed by using Eq. (17) for the trimer; *curve 4* – measured solubilization for the tetramers. **B** Curves for δ_i; numbers correspond to those in **A**

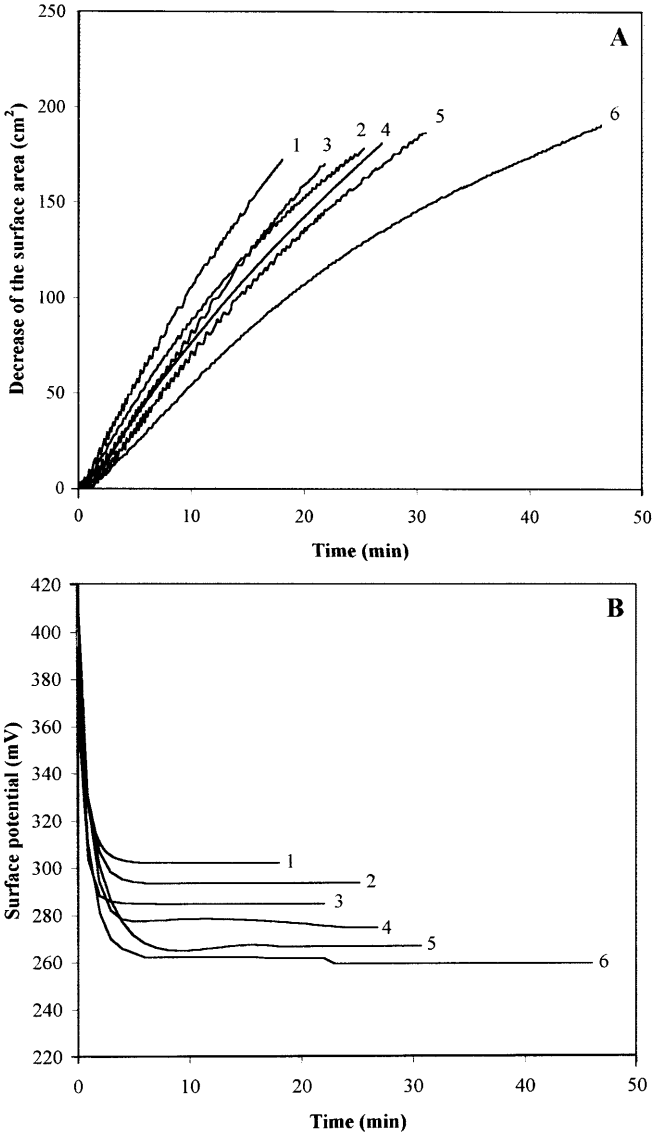

Fig. 8 Decrease in **A** the surface area (A) and **B** the surface potential ΔV with time (t) during the enzymatic hydrolysis after injection of 3 nM HLL at constant surface pressure $\pi = 5$ mNm^{-1}: *curve 1* – PCLD ($M_n = 530$); *curve 2* – PCLD ($M_n = 1250$); *curve 3* – PCLD ($M_n = 2000$); *curve 4* – PCL ($M_n = 10{,}000$), *curve 5* – PCL ($M_n = 42{,}500$), *curve 6* – PCL ($M_n = 80{,}000$). The ΔV curves presented are smoothed experimental ones

almost the same for the case of C_{13} and C_{12} (Table 1); therefore, for the trimer one could use the value of the criterion for insolubility corresponding to C_{12}, i.e., 9.9. In a similar way, φ_2 for the dimer is lower by 11.2% than φ_3, corresponding approximately to the difference between C_{12} and C_{11}. The percentage difference between φ of the dimer and the monomer corresponds to that between C_{11} and C_7, i.e., one can use for the monomer the value of the insolubility criterion for the C_7 fatty acid.

By substituting the values for the insolubility criterion in Eq. (17), one can reconstruct the $\Delta A(t)$ curves for dimers and trimers. The results are presented together with the measured curves for the monomer and tetramer in Fig. 7A. From curves 2 and 3 and Eq. (18) one obtains the estimation for $\delta_2(t)$ and $\delta_3(t)$, presented together with the measured $\delta_1(t)$ and $\delta_4(t)$ in Fig. 7B.

This concept provides the background for the calculation of the degree of completion of hydrolysis, α, under the action of HLL.

Hydrolysis kinetics

The decrease in the area and the change in the surface potential were recorded simultaneously during interfacial hydrolysis at various constant surface pressures for all polyester monolayers. The kinetics data $-\Delta A(t)$ and $\Delta V(t)$, at $\pi = 5$ mNm^{-1} and $C_{HLL} = 3$ nM, for the all PCL and PCLD monolayers studied are presented in Fig. 8A and B, respectively.

For the tetramers, the solubilization of the initially spread substrate (PCLD) should be taken into account, using the values for the relative solubilization rate, v_s, obtained from the independently measured solubilization of oligomers.

In fact, the $\Delta A(t)$ dependence is considered as a result of the solubilization of initially spread tetramers and the progressively obtained hydrolytic trimeric, dimeric and monomeric products in the reaction compartment.

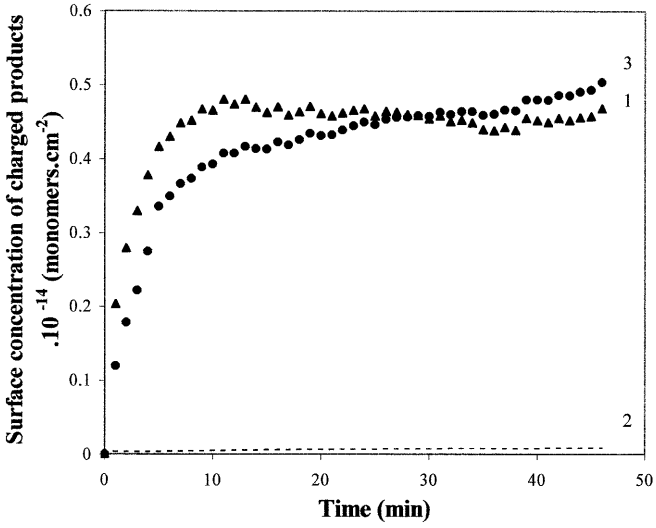

Fig. 9 Interfacial accumulation of negatively charged products during the hydrolysis of a PCL ($M_n = 80{,}000$) monolayer at $\pi = 5$ mNm^{-1} and $c_{HLL} = 3$ nM, obtained from surface pressure measurements and Eq. (2) in random mode (*curve 1*), surface pressure measurements and Eq. (2) assuming end scission (*curve 2*), and surface potential measurements and Eq. (16) (*curve 3*)

The measured decrease in the area $\Delta A(t)$ contains two contributions:

1. ΔA_s – resulting from the solubilization of the spread PCLD substrate in the reaction and reservoir compartments $\left(\Delta A_s = \Delta A'_s + \Delta A''_s\right)$.
2. ΔA_h – due to the solubilization of the hydrolytic products

$$\Delta A = \Delta A_s + \Delta A_h \ . \tag{21}$$

The first term on the right-hand side of Eq. (21) is given, at every moment, by

$$\Delta A_s = \int_{t=0}^{t} v_s A(t) \mathrm{d}t \ . \tag{22}$$

In this way, from the corrected data $\Delta A_h(t)$ (accounting for the enzymatic hydrolysis) and Eq. (1) it is possible to check the experimental dependence, $\beta(t)$. From the latter, by disposing of data for $\delta_x(t)$, one can find $\alpha(t)$ numerically in the framework of the two limit modes of fragmentation by using Eqs. (5) and (7).

The comparison of the dependences of the interfacial density of charges on time, $s^-(t)$, i.e., Eq. (2) based on $\Delta A(t)$ measurements and the electrical approach, Eq. (14), allows one to find the more probable mode of scission of long macromolecules when the two modes can be easily discriminated. s^-(t) calculated by means of Eq. (2) and the expressions for $\gamma(t)$ corresponding to the random (curve 1) or end (curve 2) scission modes are displayed in Fig. 9.

Curve 3 in the same figure is obtained by using the experimental data for $\Delta V(t)$ and the more realistic form of the Graham equation (Eq. 16) with the reasonable value of $\Delta\mu_\perp = 230$ mD. The $s^-(t)$ dependence obtained is closer to the random scission mode. It should be noted that the attempt to describe the chain-end scission (curve 2) by means of Eq. (16) requires the use of the quite unrealistic value of $\Delta\mu_\perp = -20{,}000$ mD. Therefore, the use of the random scission mode of fragmentation in the theoretical approach of the mechanism of hydrolysis of PCL is a good first approximation.

The results for the degree of completion of hydrolysis, $\alpha(t)$, for all the polymers studied, under the action of HLL in the framework of the random scission mode are presented in Fig. 10. It is seen that after 15 min, α seems to reach saturation, at approximately $\alpha = 0.8$.

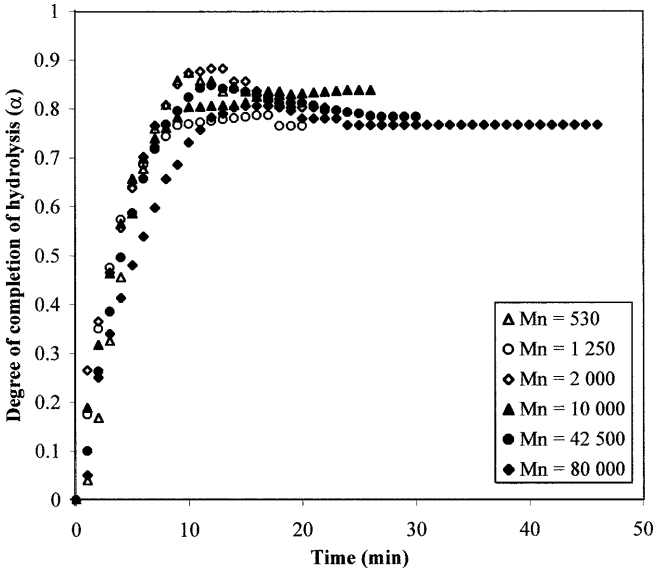

Fig. 10 Degree of completion of the hydrolysis (α) with time (t) obtained numerically (see text) for all the polymers studied

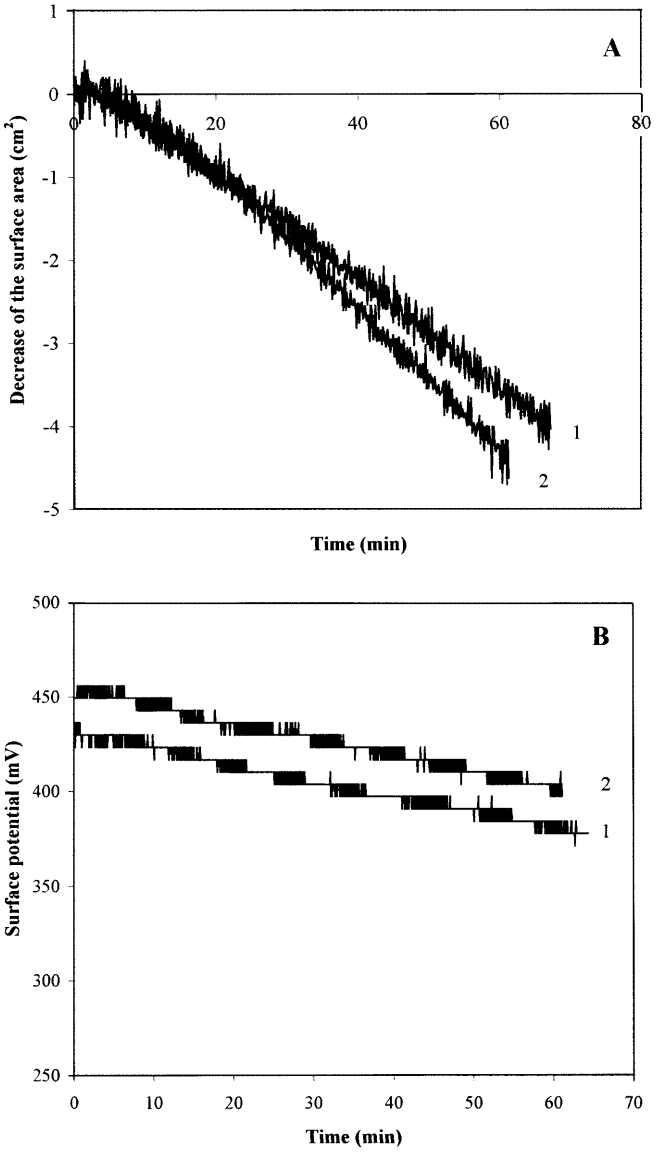

Fig. 11 Decrease of **A** the surface area (A) and **B** the surface potential ΔV with time (t) for monolayers of PCLs, after injection of 3 nM mutant HLL – S146 A at $\pi = 5$ mNm^{-1}: *curve 1* – $M_n = 10{,}000$ and *curve 2* – $M_n = 42{,}500$

Table 3 Initial interfacial turnover, SA^*_{ini}, of *Humicola lanuginosa* lipase (c = 3 nM) on various substrate monolayers, at constant surface pressure π = 5 mN m^{-1}

Substrate	M_n	SA^*_{ini}
Polycaprolactone	530	3140
	1250	5140
	2000	5550
	10,000	5340
	42,500	4135
	80,000	3760
Poly(lactic-*co*-glycolic acid)	6217	3295
Poly(lactic acid)	32,000	~0

Taking into account the reproducibility of the experiments, it is hard to determine the dependence of the kinetics $\alpha(t)$ on the chain length. Nevertheless, it seems that the kinetics slows at longer length. The flexibility of the macromolecules may be involved in the mechanism of formation of the substrate–enzyme complex and affects the hydrolytic rate.

The classical way to express the specific hydrolysis rate is the so-called turnover, defined as $SA = \frac{1}{c_{E_0}} \frac{dc_p}{dt}$, where c_{E_0} is the bulk concentration of the enzyme and c_p is the bulk concentration of the products. Taking into account that the reaction occurs at the interface (an adaptation to heterogeneous catalysis) an ''interfacial'' specific activity can be defined as

$$SA^* = \frac{1}{\Gamma_{E^*}} \frac{d\Gamma_s}{dt} \equiv \frac{\Gamma_0}{\Gamma_{E^*}} \frac{d\alpha}{dt} \quad , \tag{23}$$

where $\Gamma_{E^*}(t) = \frac{\Delta A_{enz}(t)}{a_{enz}}$ is the interfacial concentration of the enzyme (a_{enz} is the molecular area occupied by one enzyme molecule). By using the data obtained for $\alpha(t)$ in the random scission mode, the value for the interfacial specific activity of HLL (interfacial turnover), SA*, can be calculated.

The necessary information for $\Delta A_{enz}(t)$ is taken from independent measurement of the penetration of the HLL-S146 A mutant (Fig. 11) in the polyester monolayer, assuming that the surface tensioactivity for both HLL is the same. The observed changes in $\Delta A(t)$ (Fig. 11A) and $\Delta V(t)$ (Fig. 11B) are due to the penetration and adsorption of the enzyme molecules at the interface. As an illustration, the values for the initial SA* are given in Table 3.

Typical values of the specific activity of HLL on poly(lactic acid) (PLA50) and poly(lactic-*co*-glycolic acid) (PLA25GA50) as substrates at $\pi = 5$ mNm^{-1} are also presented in Table 3. The SA* of HLL on PCL is comparable with that on PLAGA substrates, while the specific activity on PLA50 is negligibly low. One can assume that the CH_3 group is responsible for the unfavourable PLA steric contact with the active site of the enzyme compared to the hydrogen atom in the cases of PGA and PCL.

In general, the specific activity of HLL on polyester substrates is much lower than on monolayers of simple molecules of di- and triglycerides (of an order of magnitude of 60,000).

In conclusion, the independent study of model monolayers containing lower-molecular-weight PCLDs allows us to test independently the solubilization of small products, assumed previously as practically instantaneous. By taking into account the values of the relative solubilization rates obtained, it is possible to determine, without any additional supposition, the kinetics of the enzymatic reaction.

At this stage, the choice of our approach is restricted by the specific difficulties the classical methods (mass spectroscopy, size-exclusion chromatography, etc.) entail in following the course of the hydrolytic reaction when the polymer substrate is in the form of a monolayer at the air–water interface. The comparison of our results with those obtained by classical methods for monitoring the polymer degradation process will be the object of future investigations.

Acknowledgements This work was partially funded by the Bulgarian National Foundation for Scientific Research and by EU Project BIOTECH PL 98–2365.

References

1. Vert M (1986) In: Buck S (ed) CRC critical reviews – Therapeutic drug carrier systems, vol 2. CRC, Boca Raton, p 291
2. Lewis DD (1990) In: Chasin M, Langer RS (eds) Biodegradable polymers as drug delivery systems. Dekker, New York, p 1
3. Mauduit J, Vert M (1993) STP Pharm Sci 3:197
4. Chu CC (1982) J Biomed Mater Res 16:117
5. Makino K, Arakawa M, Kondo T (1985) Chem Pharm Bull 33:1195
6. Makino K, Ohshima H, Kondo T (1986) J Microencapsul 3:203
7. Coffin MD, Mc Ginity W (1992) Pharm Res 9:200
8. Chu CC, Williams DF (1983) J Biomed Mater Res 17:1029
9. Koetsu I, Yoshida M, Asano M, Yamanaka H, Imai K, Yuasa H, Mashimo T, Suzuki K, Katakai R, Oya M (1987) J Controlled Release 6:249
10. Vert M, Li S, Garreau H (1991) J Controlled Release 16:15
11. Fukuzaki H, Yoshida M, Asano M, Kumakura M, Mashimo T, Yuasa H, Imai K, Yamanaka H (1991) Biomaterials 12:433
12. Spenlehauer G, Vert M, Benoit JP, Boddaert A (1989) Biomaterials 10:557
13. Holland SJ, Tighe BJ, Gould PL (1986) J Controlled Release 4:155
14. Göpferich A (1996) Biomaterials 17:103
15. Batycky RP, Hanes J, Langer R, Edwards D (1997) J Pharm Sci 86:1464
16. Shih C (1995) J Controlled Release 34:9

17. Ivanova T, Panaiotov I, Boury F, Proust JE, Benoit JP, Verger R (1997) Colloids Surf B 8:217
18. Ivanova T, Grozev N, Panaiotov I, Proust JE (1999) Colloid Polym Sci 277:709
19. Ivanova T, Svendsen A, Verger R, Panaiotov I (2000) Colloid Polym Sci 278:719
20. Ringard-Lefebre C, Baszkin A (1994) Langmuir 10:2376
21. Verger R, de Haas G (1973) Chem Phys Lipids 10:127
22. Davies JT, Rideal EK (1961) Interfacial phenomena. Academic, New York
23. Ward AFH, Tordai L (1946) J Chem Phys 14:453
24. (a) Boury F, Olivier JE, Proust JE, Benoit JP (1993) J Colloid Interface Sci 160:1; (b) Boury F, Olivier JE, Proust JE, Benoit JP (1994) J Colloid Interface Sci 163:37
25. Boury F, Gulik A, Dedieu JC, Proust JE (1994) Langmuir 10:1654
26. (a) Boury F, Ivanova T, Panaiotov I, Proust JE, Bois A, Richou J (1995) J Colloid Interface Sci 169:380; (b) Boury F, Ivanova T, Panaiotov I, Proust JE, Bois A, Richou J (1995) Langmuir 11:1636
27. Panaiotov I, Dimitrov DS, Ivanova MG (1979) J Colloid Interface Sci 69:318